REPORT DOCUMENTATION PAGE AFRL-SR-AR-TR-03-

0074

viewing
rmation

1. AGENCY USE ONLY *(Leave blank)*

2. REPORT DATE

3. REPORT TYPE AND DATES COVERED
01 Jun 96 to 30 Sep 99 FINAL

4. TITLE AND SUBTITLE
Ultralow Threshold Semiconductor Lasers based on Gain without Inversion

5. FUNDING NUMBERS
61102F
2305/DX

6. AUTHOR(S)
Professor Malloy

7. PERFORMING ORGANIZATION NAME(S) AND ADDRESS(ES)
UNIVERSITY OF NEW MEXICO
OFFICE OF RESEARCH ADMIN
SCHOLES HALL 102
ALBUQUERQUE NM 87131-6003

8. PERFORMING ORGANIZATION REPORT NUMBER

9. SPONSORING/MONITORING AGENCY NAME(S) AND ADDRESS(ES)
AFOSR/NE
4015 WILSON BLVD
SUITE 713
ARLINGTON VA 22203

10. SPONSORING/MONITORING AGENCY REPORT NUMBER
F49620-96-1-0325

11. SUPPLEMENTARY NOTES

12a. DISTRIBUTION AVAILABILITY STATEMENT
APPROVED FOR PUBLIC RELEASE, DISTRIBUTION UNLIMITED

12b. DISTRIBUTION CODE

13. ABSTRACT *(Maximum 200 words)*

Quantum interference effects in semiconductors for use in the active regions of low threshold lasers. Quantum interference lies behind electromagnetic induced transparencies and gain without inversion in three level systems. Achieving this behavior in reduced dimensionality semiconductor quantum systems opens a host of potential applications and devices. Experiments in atomic systems and modeling of semiconductors has established the conditions and configurations necessary for these phenoment The initial portion of our proposed work expands our theory and modeling and performs experimental investigation of the optical properties of various quantum interference configurations. We plan to add time dependence and many-body effects to our theory and plan to investigate optical and intrinsic coupling configurations experimentally. For low threshold lasing, we will investigate the possibility of excitonic lasing without inversion in semiconductor quantum wells based on the AlGaInAs materials system. Both interband and intraband lasers will be investigated.

20030326 023

14. SUBJECT TERMS

15. NUMBER OF PAGES

16. PRICE CODE

17. SECURITY CLASSIFICATION OF REPORT	18. SECURITY CLASSIFICATION OF THIS PAGE	19. SECURITY CLASSIFICATION OF ABSTRACT	20. LIMITATION OF ABSTRACT
UNCLASSIFIED	UNCLASSIFIED	UNCLASSIFIED	UL

Final Report

1. ABSTRACT

We propose to investigate the quantum interference effects in semiconductors for use in the active regions of low threshold lasers. Quantum interference lies behind electromagnetic induced transparencies and gain without inversion in three level systems. Achieving this behavior in reduced dimensionality semiconductor quantum systems opens a host of potential applications and devices. Experiments in atomic systems and modeling of semiconductors has established the conditions and configurations necessary for these phenomena. The initial portion of our proposed work expands our theory and modeling and performs experimental investigation of the optical properties of various quantum interference configurations. We plan to add time dependence and many-body effects to our theory and plan to investigate optical and intrinsic coupling configurations experimentally. For low threshold lasing, we will investigate the possibility of excitonic lasing without inversion in semiconductor quantum wells based on the AlGaInAs materials system. Both interband and intraband lasers will be investigated.

2. TECHNICAL BACKGROUND

While the utility of semiconductor lasers is beyond dispute, some disadvantages remain. In particular, the appearance of a threshold to lasing, and hence an operating nonlinearity, complicates circuit and system applications. The absence of a threshold in the lowly LED makes that device useful in some low-cost communications links. The response of the semiconductor laser device physicists has been to seek to minimize the threshold so as to render the nonlinearity invisible to the circuit. Thus far, only one approach to ultra-low threshold lasers with proven results exists. By vigorously minimizing the volume of the active region, the concentration of carriers necessary to reach transparency is minimized. Almost always, these active regions are accompanied by very high quality factor cavities, thus minimizing loss and hence the threshold current levels. Examples include quantum well edge emitting lasers with high reflectivity dielectric coatings, vertical cavity surface emitting lasers where processing minimizes active region volume and multilayer semiconductor DBRs minimize loss, and microdisk lasers with extremely small cavity volumes. Such techniques have resulted in thresholds as low as 100 μA. However, small laser volumes do have some restrictions. The output from such a laser is severely limited. The lasers still exhibit spontaneous emission noise and hence make poor amplifiers. The dynamic range and onset of nonlinearities compromises system designs. Optical mode control remains an issue.

We propose a completely new approach to ultra-low threshold lasers using quantum mechanical interferences to establish transparency at equilibrium. Gain then occurs with the first carrier pair injected. Such a condition is called lasing without inversions and differs in a fundamental way from approaches such as inhibited spontaneous emission or single oscillator microlasers.

Lasing without population inversion can result from the combined effects of Fano interference and coherent superposition [Harris 1989], [Scully 1989]. As first steps toward inversionless lasing, electromagnetically induced transparency and gain without population inversion has recently been observed in atomic systems [Boller, Imamoglu, & Harris 1991], [Fry et al. 1993]. Since lasing without inversion has obvious scientific and technological implications, we initiated studies of the possibilities of similar phenomena in semiconductor quantum confined structures [Lee & Malloy 1994].

Our work reveals the Fano interference configuration has the possibility of exhibiting gain without inversion in semiconductor quantum structures. Therefore, this proposal focuses on the

observation and exploitation Fano-interference in semiconductors. Gain without inversion is introduced by first reviewing the basic concepts in atomic systems, and then by describing the analogous extensions to semiconductor quantum structures. Quantum interference effects such as zero absorption, gain without inversion, and inversionless lasing in semiconductor quantum structures are proposed for investigations eventually leading to practical applications. As described below, our first step is to investigate the circumstances necessary for zero absorption before proceeding to gain without inversion and lasing. Possible applications related to ultralow threshold lasers include optical amplifiers, inversionless laser diodes, unipolar far-IR lasers, and even microlaser diodes using excitonic lasing Other applications such as ultrafast modulators, group velocity compensators, nonlinear generation are also discussed.

2.1 Why Gain without Population Inversion in Semiconductors

Normally, absorption and emission are symmetric, inverse processes and gain only occurs if a population inversion is achieved. Lasing results from the combined effects of this gain and feedback of the amplified signal. If destructive quantum mechanical interference occurs for absorption, but not emission, the symmetry between absorption and emission is removed and potentially, all transitions result in emission, and lasing efficiency approaches unity. To achieve this, zero absorption must first exist, then a properly injected excited carrier population will result in lasing. That is, gain without inversion based on zero absorption can make the lasing efficiency approach unity. Zero absorption, with unaltered, but narrow linewidth emission processes is the path we plan to pursue leading to gain without inversion.

Population inversion itself implies the existence of an input threshold for lasing and spontaneous emission noise. Gain without population inversion makes possible thresholdless lasing or optical amplification, and single carrier and single photon microlasers with unit efficiency. By removing the restrictions of population inversion for lasers and optical amplifiers, thresholdless lasers and optical amplifiers, single carrier microlasers, and noiseless lasers become possible.

Atomic systems demonstrate electromagnetically induced transparency by exhibiting a narrow window of zero absorption. This may be introduced using DC electric fields or by using coherent superposition by optical pumping. Because atomic systems have clearly defined energy levels and almost always deal with only single electron transitions, the basic principles of zero absorption and gain without inversion are well illustrated. However, utilizing atomic systems requires a large and complicated apparatus, almost eliminating practical systems. Semiconductor quantum structures, while easily converted into practical devices, have complicated energy band

structures and exhibit many body effects as well. This proposal makes use of two factors to overcome the disadvantages of semiconductors: first, the technological achievements embodied by the term "bandgap engineering" vastly increase the configurations and physical principles that can be exploited in semiconductors and second, the very existence of large electron concentrations in semiconductors implies both high gain and a large response when zero absorption is established. We first discuss the basic physics of zero absorption and gain without inversion and then follow with detailed semiconductor configurations .

2.2 Origination from Atomic Systems

Lasing without inversion requires gain without population inversion. Replacing absorption with gain without using population inversion requires quantum interference. Consider the configuration shown in Fig. 3.1, consisting of a stable ground state and metastable and unstable (in terms of their relative lifetimes) excited states. Electromagnetic or electric field coupling between the two excited states results in Rabi splitting (or equivalently, the optical or DC Stark effect), creating unbalanced lifetime dressed states. Destructive quantum interference (a subset of the physical processes that occur in Fano interference) can then occur for transitions between the stable state and these unstable, coupled states in analogy with two-slit quantum interference. Therefore, a three level system consisting of one stable ground state and one pair of excited states (one metastable and one unstable) is the canonical system for observation of zero absorption. Electromagnetic or electric field coupling between two excited states and the resulting quantum interference between the unstable excited states and a ground state are shown in Fig. 3.1. Creating unbalanced dressed states by mixing an unstable state and a metastable state with a coupling field of the proper strength is the fundamental phenomena we seek to exploit.

For example, Sr, Pb, and Zn vapors have shown electromagnetically induced transparencies, and the atomic hydrogen system has demonstrated electrically induced transparency for second harmonic generation [Hakuta, Marmet, & Stoicheff 1992]. Electromagnetically induced transparency has been shown first for nonlinear processes in Zn vapor, followed by linear processes in Sr and Pb atomic systems [Hahn, King, & Harris 1990]. In nonlinear generation, the electromagnetic or electric couplings creates a zero absorption window for propagating generated signals without reducing the nonlinear generation emission processes. Since the optical or electrical fields need be resonant with the atomic levels, however, matches between these couplings and convenient sources have limited the investigation of atomic systems. All these conditions make observation of gain without inversion in atomic systems difficult using electromagnetic or electric field coupling.

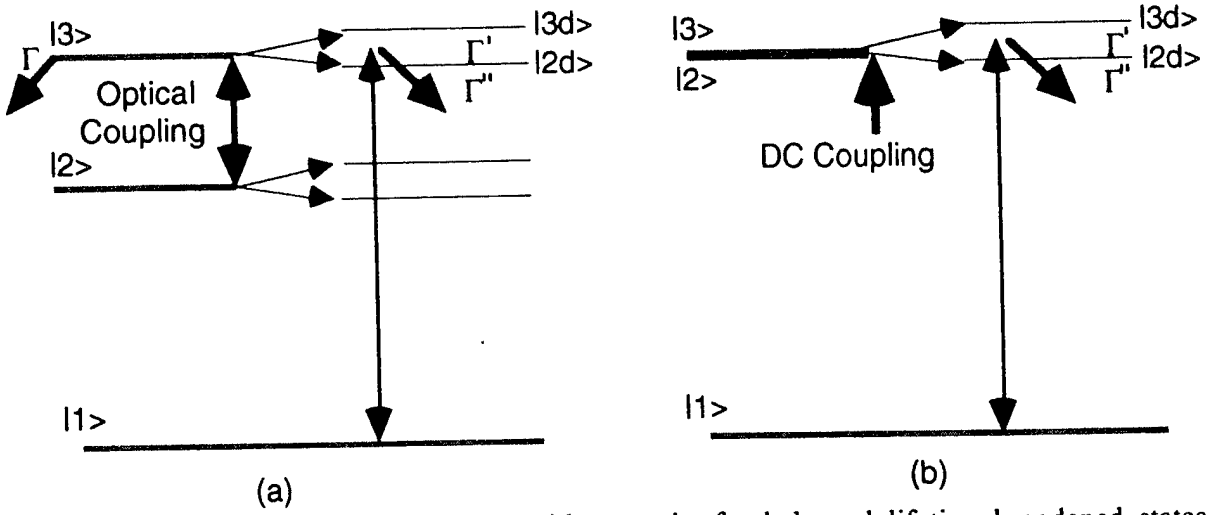

Figure 3.1 Three level atomic system with one pair of unbalanced, lifetime broadened, states.
(a) shows the formation of dressed states through optical coupling.
(b) shows the "dressed" states occurring when degenerate states are split by DC coupling.

Unlike electromagnetically induced configurations, coherent superposition systems have shown gain without population inversion [Nottelmann, Peters, & Lange 1993], [Fry et al. 1993], [van der Veer et al. 1993]. Coherent superposition configurations originated from the so-called "quantum beat" lasing schemes, and have been studied enough to demonstrate gain without inversion. However, they rely on sensitive control of the quantum mechanical phase to achieve the destructive interference, control we do not feel is achievable in solids such as semiconductors . Therefore the Fano type configurations discussed above will be investigated for semiconductors. So far all atomic systems exhibiting quantum interferences require huge input pumping fields, but produce very small outputs regardless of Fano or coherent superposition schemes. The atomic experiments have established the basic physical concepts for gain without inversion or zero absorption. Our goal is to push these investigations further by concentrating on practical, semiconductor based systems.

2.3 Atomic Systems to Semiconductor Quantum Structures

Reduced dimensionality semiconductor quantum structures are analogous to atomic systems in several ways. The density of states becomes more atomic-like by eliminating dimensional degrees of freedom. Furthermore, the exact energy spectrum and lifetimes can be controlled using the techniques loosely called "bandgap engineering." The following describes the basic properties of semiconductor structures in terms of analogous atomic systems and examines the possibility of quantum interference effects for lasing without inversion.

FUNDAMENTAL PHYSICS

- **Constructing three-level systems**

  Semiconductor quantum dots correspond exactly to zero dimensional atomic systems, but crystal growth and processing technology have not yet reached the same level of maturity represented by semiconductor quantum well technology.

  Furthermore, excitons in semiconductor are, in and of themselves analogous to atomic systems. Continuum transitions in quantum wells are included by integrating over momentum space. In addition, energy levels and lifetimes ca be controlled. The construction of a three level semiconductor quantum well system is not an issue..

- **Creating unbalanced dressed states**

  Coupling semiconductor inter-conduction-subband states results in Rabi splitting and dressed states. This is exactly analogous to the Autler-Townes effect in atomic systems. Coupling sources can be an optical field, DC electric field, or intrinsic coupling in double quantum well structures, providing more alternatives than in atomic systems.

  To create unbalanced lifetimes between the coupled states, scattering from Γ to X bands or tunneling mechanisms can be used. Thus the possibility of quantum interference effects exists for asymmetric quantum structures. [Maschke, Thomas, & Göbel 1991], [Sirtori et al. 1994].

- **Zero absorption**

  Since unbalanced dressed states are already established, selected allowed interband transitions can give transparency without absorption. If coupling effects are not large enough or lifetimes not unbalanced, transitions show only reduced absorption from Stark effects.

  Excitonic transitions are prime candidates for investigating zero absorption. Continuum interband transitions should include Fermi population distributions and integrate over all possible momentum space. Continuum effects normally result in reduced absorption without population excitation [Lee et al. 1994].

- **Gain without population inversion**

  Without nonequilibrium populations, modeling of semiconductor quantum structures shows zero absorption. Any population in excited states should result in gain without population inversion. Excited population can be provided easily in semiconductors by electrical or optical injection.

  The excitonic transition could also experience inversionless gain under low level injection before carrier densities screen the exciton binding energies. For continuum transitions, more injection, still short of inversion, is necessary. However, these injection level should screen out excitonic transitions. Therefore, either excitonic gain or continuum gain, but not both, is possible.

APPLICATIONS

- **Ultra Fast Modulator and Group Velocity Compensator**

  Optical coupling of intersubband transitions has a subpicosecond response, offering a new mechanism for a **ultra fast modulator**.

  Zero absorption occurs over very narrow frequency range. The accompanying large index changes (through the Kramers-Kronig relationship) are proportional to the slope of the absorption change. We can use this index change for **adjustable group velocity compensation** by controlling the coupling strength.

- **Nonlinear generation**

  Semiconductors usually have very large nonlinear coefficients, unfortunately accompanied by large absorption.

  By introducing intermediate states (such as defects) in our semiconductor quantum structures, nonlinear generation without radiative recombination can occur. Propagating the nonlinearly generated signal through a region of zero absorption or amplification without population inversion provides for a dramatic enhancement.

- **Optical amplifier**

  Optical amplification serves as the first test of gain without inversion. Of particular interest and importance are the noise properties of such an amplifier.

- **Lasing without inversion; Microlaser**

  Gain without inversion can operate a microlaser; a single carrier injected into a high Q factor microcavity will lase. This is different from microlaser scheme relying on inverted active medium.

- **Excitonic lasing**

  Gain without inversion leads to thresholdless lasing. If excitonic features are not screened out, the system can lase on the high density of states, narrow linewidth, excitonic features. While quantum interference-induced linewidths can approach zero using intrinsic coupling, high power lasing is unlikely. Excitonic lasers are the primary candidates for microlasers.

- **Thresholdless laser diode**

  One of our final goals will be the intrinsically coupled, electrically injected, thresholdless laser diode. Even if a truly thresholdless diode is not possible, reductions in threshold are also useful.

3. UNM'S RELATED WORK

We have investigated electromagnetically induced quantum interference in semiconductor quantum structures, and developed an electron density matrix approach for the general solution of zero absorption and gain without inversion problems in solids [Lee & Malloy 1992, 1994]. Key for lasing without inversion, electromagnetically induced transparency mechanism has been investigated in a simple symmetric semiconductor quantum well, using intersubband coupling. Our experimental results have shown reduced absorption arising from the optical Stark effect. Zero absorption has not been observed as of this time. However, our results imply the conduction subband lifetimes are long enough to observe reduced absorption at room temperature.

3.1 Development of General Density Matrix Approach

Three-level semiconductor quantum well systems have been studied by others using perturbation approaches. However, perturbation solutions either have weak field limitations or restrictions arising from complicated iterative derivations, and are cumbersome techniques for analyzing quantum interference in three-level semiconductor quantum structures. Therefore, we have developed a general density matrix approach to all three level systems for zero absorption and gain without inversion including atomic and semiconductor systems.

To understand zero absorption and gain in three-level systems, we need to extract the susceptibility from the off-diagonal density matrix elements. The equation below describes the relation between susceptibility and density matrix elements.

$$\chi(\omega) = \int f(E)\, D(E)\, [\mathbf{u}\, \rho(\omega) + \rho(\omega)\, \mathbf{u}] \,/\, \varepsilon_0 F(\omega)\, dE$$

Here f(E) and D(E) represent Fermi distribution function and density of states for semiconductors, and u, $\rho(\omega)$, and $F(\omega)$ correspond to dipole matrix elements, density matrix elements, and the transition electromagnetic field, respectively.

Three-level semiconductor quantum structures have one stable state interacting with the probing field and two excited upper states interacting with the coupling field. The following electron density matrix equation describes the semiconductor quantum structures under probing and coupling interactions treating relaxations as phenomenological scattering terms

$$\frac{\partial \rho}{\partial t} = \frac{1}{i\hbar}[(\boldsymbol{H_0} + \boldsymbol{H_I}), \rho] - \frac{1}{2}(\Gamma\rho + \rho\Gamma),$$

where $\boldsymbol{H_0}$ and $\boldsymbol{H_I}$ are the intrinsic Hamiltonian and coupling Hamiltonian, ρ is a density operator with ρ_{ij} density matrix elements, and Γ is the diagonal matrix determined by the inverse of the relaxation time τ_i for each state $|i\rangle$.

The electron density matrix can be solved exactly in terms of the diagonal population distribution matrix elements. The exact general steady state solutions in the frequency domain are as follows

$$\rho_{cb}(\omega_p) = \frac{(D_{db}D_{dc} - |\Omega_{cb}|^2)\Omega_{cb}(\rho_{bb} - \rho_{cc}) - \Omega_{cb}|\Omega_{cd}|^2(\rho_{cc} - \rho_{dd})}{D_{cb}(D_{db}D_{dc} - |\Omega_{cb}|^2) - D_{dc}|\Omega_{cd}|^2}$$

where the subscript b refers to the stable state, the subscripts c and d correspond to upper states, ω_p, the probing frequency, $\Omega_{ij}=u_{ij}F/\hbar$ represent couplings, and $D_{ij}=[\omega-(E_i-E_j)/\hbar]+i\gamma_{ij}$ with $\gamma_{ij}=(\Gamma_{ii}+\Gamma_{jj})/2$. Since intersubband coupling results in dressed states and therefore serves as a population trapping mechanism, we can assume constant population distributions [Boyd 1992], [Cohen-Tannoudji, Diu, & Laloë 1977]. If there is no coupling or $\Omega_{cd}<<\Omega_{cb}$, the solution is equivalent to a simple two level resonant transition (as a way of checking validity of the derivation),

$$\rho_{cb}(\omega_p) = \frac{\Omega_{cb}(\rho_{bb} - \rho_{cc})}{D_{cb}}$$

When the population of ground state, ρ_{bb}, is dominant and taken as unity, the population of the upper states ρ_{cc} and ρ_{dd} have values close to zero, and $\Omega_{cd}>>\Omega_{cb}$ for the case of a weak probe field, the final simplified steady state solution under probing has the same form as iterative perturbation results

$$\rho_{cb}(\omega_p) = \frac{D_{db}\Omega_{cb}}{D_{cb}D_{db} - |\Omega_{cd}|^2}$$

Under weak probe fields, both formulas give the same result. However, for emissive process such as gain without inversion, the solution must include all terms. Neglecting excited carriers results in the same solution as the iterative perturbation result but fails to show emission processes. Therefore our exact solution is needed to include gain effects in the general configuration.

3.2 Investigation of Optical Stark Effects in Semiconductors

Intersubband coupling effects have been studied in symmetric semiconductor quantum well [Fröhlich et al. 1987], [Lee et al. 1994]. Results from our density matrix approach predict reduced absorption (arising from Rabi splitting) as a consequence of the optical Stark effect.

Zero absorption from destructive quantum interference does not occur since the symmetric quantum well does not have unbalanced conduction subband lifetimes . Our experiments have confirmed the reduced absorption, and revealed the conduction subband lifetime as long enough to observe the optical Stark effect at room temperature. This lifetime observation is key to the next step towards zero absorption and gain without inversion.

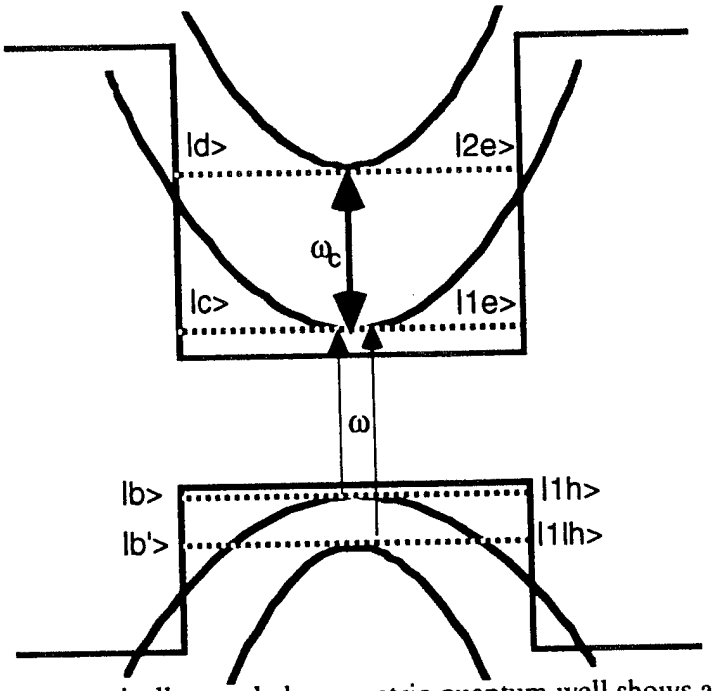

Figure 3.1 Electromagnetically coupled symmetric quantum well shows all possible transitions on the bandedge of k_z with parabolic bands of k_x and k_y.

Our experiment was performed on a multiple quantum well structure consisting of 65 pairs of 8.5 nm GaAs quantum wells and 23.2 nm $Al_{0.3}Ga_{0.7}As$ barriers. Figure 3.1 describes the single quantum well structure under coupling and probing fields. Since we have derived the steady state susceptibility, the experiment uses long coupling laser pulses and white light probing giving time independent results. Figure 3.2.(a) shows the absorption profiles as a function of coupling strength (by controlling boxcar time delays with respect to the variable intensity coupling laser pulse). The result indicates that the moderate coupling strength (20 kw/cm^2) can be enough to show evidence of the optical Stark effect. In other words, the conduction subband lifetimes are long enough (<10 ps) at room temperature to exhibit reduced absorption. However, we still need to increase the coupling laser power to construct clear Rabi splitting, which requires coupling strength comparable to conduction subband lifetimes. Our coupling laser did not have enough power to investigate the exact lifetimes of conduction subbands. The exact lifetime includes all possible broadening factors such as quantum well thickness variations as well as unexpected lifetime factors such as thermal effect due to substrate absorption (fortunately, thermal effects

occur at longer times and can be gated out). Our main result, 1-10 ps subband lifetimes as extracted value from the moderate 20 kw/cm^{2}coupling strength, confirm the possibility of measuring subband lifetime at room temperature using the combined effects of the optical Stark effect and the large excitonic binding energy.

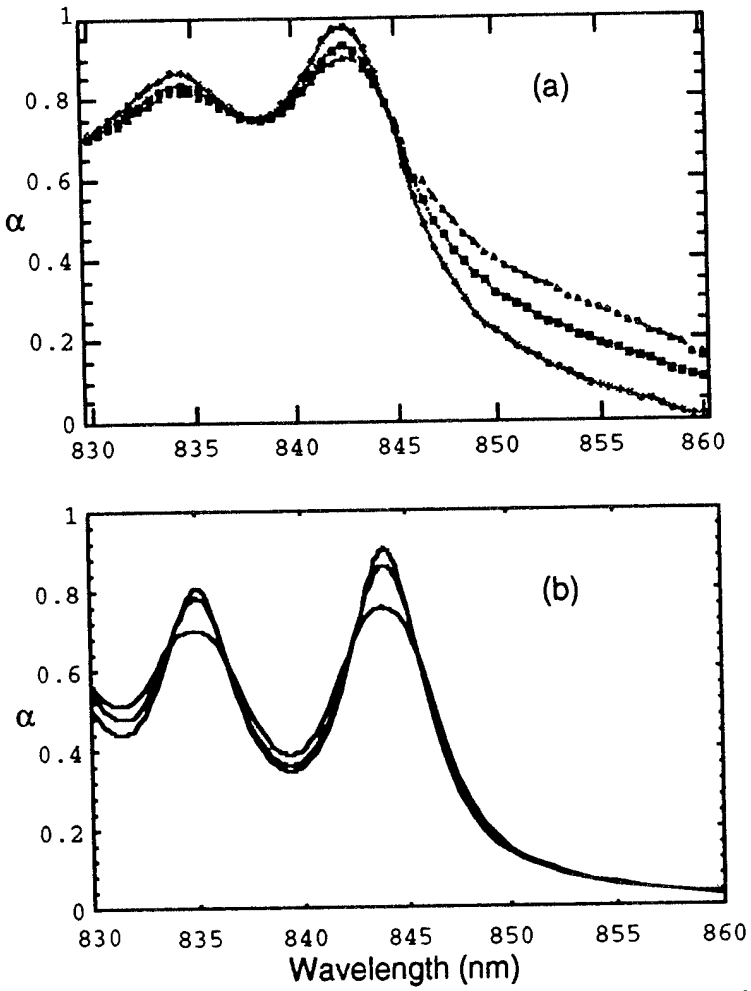

Figure 3.2 Optical Stark effect from 8.5 nm GaAs quantum well shows reduced absorption.
(a) Measured absorption profiles of the 65 multiple quantum well structure.
(b) Calculated absorption profiles of the single quantum well structure.

As semiconductor quantum wells have both excitonic and continuum transitions, Fig.3.2.(b) shows the calculated overall absorption profile results as a function of intersubband coupling strength, in a single symmetric quantum well of 8.5 nm GaAs. Our simulation result points that the reduced absorption mechanism begins to appear when the coupling field is comparable to intersubband scattering. Overall, the modulation of continuum absorption is not readily distinguishable from other modulated signals, but the heavy hole excitonic transition can be observed separately. These calculations are reasonably well matched with the experimental result

shown Fig.3.2.(a) under moderate coupling strength. Heavy and light hole absorption peaks are gradually reduced as coupling strength is increased. However because of the limit of our coupling laser power, background normalization effects , and thermal effects, we don't show clear Rabi splitting at this time. While our simulation results are close to the experimental results, we still need to explain various broadening factors and exciton binding energies. An important difference between the experiment and calculation is the number of quantum wells. The multiple quantum well usually enhances the signal, but inhomogeneous broadening obscures the response.

4. PROPOSED CONFIGURATIONS

We have described the symmetric semiconductor quantum well optical Stark effect configuration. The lack of unbalanced lifetimes for the excited states results in only reduced absorption. To achieve zero absorption through quantum interference, we need to unbalance the conduction subband lifetimes using tunneling or band mixing effects [Faist et al. 1994], [Maschke, Thosmas, & Göbel 1991]. We plan to investigate asymmetric quantum well structures for this purpose [Lee et al. 1995]. Asymmetric structures not only provide unbalanced conduction subband lifetimes, but also permit control of background absorption by reducing the oscillator strength of the supporting transitions. As we shall see, tunneling or band mixing-induced scattering mechanisms then provide the unbalanced, subband lifetimes, which in turn, establishes nonreciprocal decay paths for zero absorption. At this time, it appears that the tunneling mechanism requires slightly more complicated structures. Therefore, we will first investigate the band mixing mechanism for unbalanced lifetimes. In addition, asymmetric quantum structures will still have some background absorption from perpendicular momentum continuum transitions. (To avoid background absorption altogether, quantum dots instead of quantum wells could be used, but the technology for making uniform quantum dots falls considerably short of quantum well quality). This section first describes a simple asymmetric quantum structure comparable to an electromagnetically coupled atomic system, then describes replacing optical coupling by intrinsic coupling. Finally, we discuss applications of these configurations to optical amplifiers and lasing without inversion, microlasers, optical modulators, group velocity compensators, and nonlinear sources.

4.1 Electromagnetically Coupled Configurations

Since electromagnetically induced transparency has been observed in atomic systems, we have investigated similar phenomena in an asymmetric quantum structure. To achieve the

unbalanced lifetime combination without background continuum absorption, we designed a special asymmetric quantum structure using band mixing-induced scattering. Calculated results shows zero absorption for excitonic transition without population of the excited energy levels. Slight population of the excited states results in gain without inversion for both excitonic and continuum transitions.

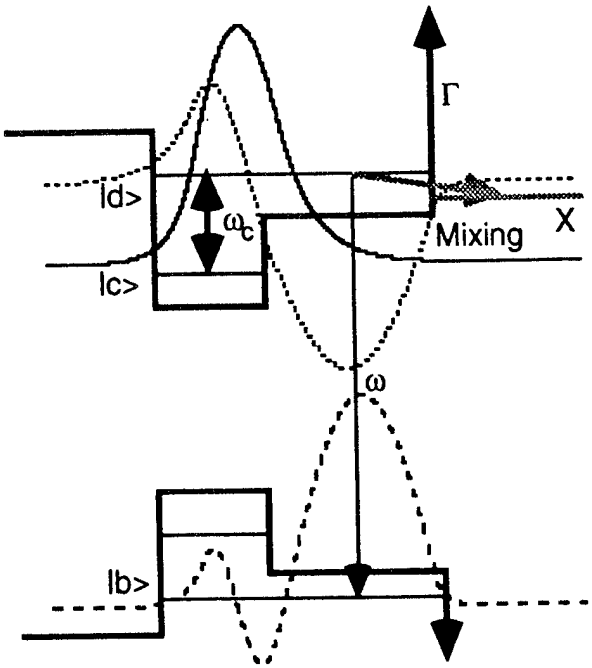

Figure 4.1 Electromagnetically coupled asymmetric quantum well configuration with envelop wave functions and an optional band mixing decaying path.

Figure 4.1 describes an asymmetric semiconductor quantum well showing each energy level's envelope wave functions. Strong overlap occurs for both interband and intersubband transitions. The asymmetric quantum well consists of a lower barrier layer of $Al_{0.5}Ga_{0.5}As$, a 5 nm $Al_{0.25}Ga_{0.75}As$ narrow quantum well region and a 10 nm wide $Al_{0.4}Ga_{0.6}As$ quantum well, and a higher barrier layer of AlAs to permit band mixing-induced scattering. If band mixing-induced scattering is not necessary and all direct bandgap material can be used, the Al composition ratio in each layer can be reduced by 0.25. The asymmetric quantum well configuration provides for a Γ-X band mixing-induced scattering mechanism that results in fast, nonreciprocal decay paths for the destructive quantum interferences. The alternative to band mixing scattering is a tunneling structure where the lifetime is controlled by the thickness of the tunneling barrier. Since the asymmetric quantum well results in an n=1 metastable conduction subband energy state in the narrow side of the well and an n=2 unstable energy state in the wide side, as shown in Fig. 4.1, the strongest transition happens between the n=2 intersubband states with unbalanced lifetime resulting from optical coupling of the n=1 and n=2 conduction subband

states. The asymmetric configuration also reduces the background absorption problem by using wide active quantum well region for good overlap of the n=2 envelope wave functions as opposed to the n=1 narrow "well" transition.

The system can be pumped optically or electrically. Both cases result in zero absorption without excited carriers or gain without population inversion upon slight carrier excitation as shown in Fig. 4.2. Unlike the symmetric quantum well, destructive quantum interference results in a narrow transparency and gain window.

With few carriers in the conduction subbands, Fig. 4.2.(a) reveals zero absorption and the possible application as a fast optical modulator control by intersubband coupling. This ***excitonic modulator*** *works on distinctly different principles than such modulators as SEEDs relying on excitonic saturation.*

If we inject a few carriers, the system exhibits gain without population inversion on the excitonic transitions. Therefore, before the carrier concentration is large enough to screen the excitons, excitonic modulation or excitonic lasing is possible. Unlike typical laser diodes, this mechanism provides a very narrow gain profile and high conversion efficiency from the larger exciton oscillator strength than continuum transition as shown in Fig. 4.2.(b). This configuration can be applied to an ***excitonic microlaser****.*

For strong injection still short of population inversion, excitonic transitions are screened out, and continuum transitions dominate. The continuum transitions can be used also for modulators, but lasing can also be anticipated. Since continuum absorption occurs over all possible momentum space, we need more injection to achieve and get a broader gain profile. Figure 4.2.(c) describes the continuum gain profile. Again, this gain profile can be applied to ***lasing without inversion****.*

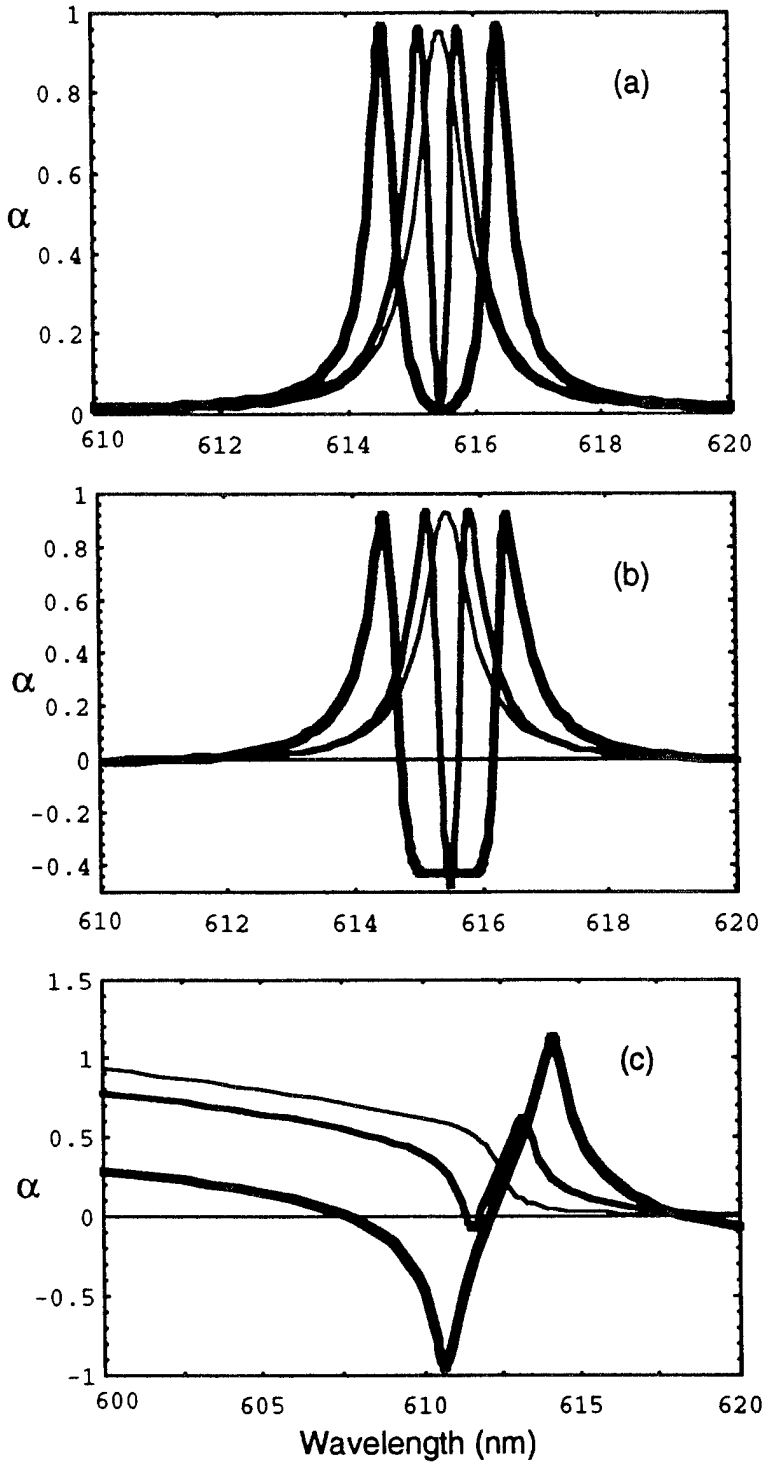

Figure 4.2 Absorption profiles in the electromagnetically coupled asymmetric quantum well as a function of coupling strength from 0 meV to 3 meV for excitonic transitions and 0 meV to 6 meV for continuum transitions, proportional to line thicknesses.
(a) Excitonic probing as a function of coupling strength.
(b) Excitonic transition for gain without population inversion.
(c) Continuum transition for gain without population inversion.

4.2 Intrinsically Coupled Configurations

Optical coupling in the asymmetric quantum well has revealed promising characteristics. In order to ensure relevance to device applications, the optical coupling mechanism can be replaced by intrinsic coupling by inserting a thin barrier in the asymmetric quantum well, . While optical coupling configurations are analogous to electromagnetically coupled atomic systems, intrinsic coupling configurations are analogous to DC-coupled degenerate atomic systems. For device applications, the DC coupling and electrical injection might both arise from the same external bias. However, undertaking such a combined problem is currently beyond our capabilities. Instead of DC-field coupling, we plan to investigate intrinsic coupling arising from a double quantum well barrier. Intrinsic coupling itself requires complete consideration of energy levels and coupling strengths, but it provide the flexibility necessary for controlling electrical injection and transition frequencies simultaneously.

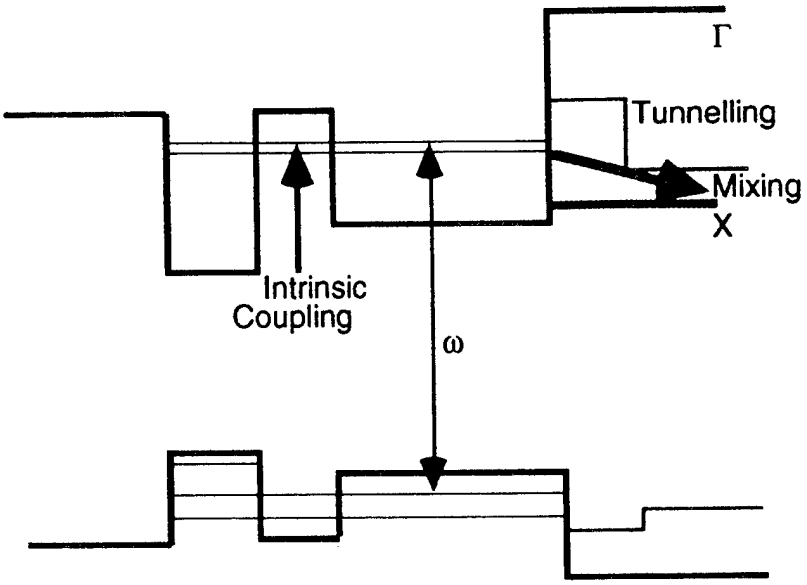

Figure 4.3 Intrinsically coupled asymmetric double quantum well configuration with tunneling or band mixing decay path.

Figure 4.3 shows intrinsic coupling in an asymmetric double quantum well. The electromagnetically coupled configuration is modified by inserting an intrinsic coupling barrier in the asymmetric quantum well region. The instrinsically coupled asymmetric double quantum well consists of a lower barrier of $Al_{0.5}Ga_{0.5}As$, a narrow quantum well of 2.5 nm $Al_{0.25}Ga_{0.75}As$ and a wide quantum well of 7.0 nm $Al_{0.35}Ga_{0.65}As$ with a 2.5 nm $Al_{0.5}Ga_{0.5}As$ coupling barrier, and a higher barrier of AlAs for band mixing-induced scattering or a adjustable tunneling barrier of $Al_{0.5}Ga_{0.5}$ with a $Al_{0.37}Ga_{0.63}As$ lower spacer to control the lifetimes of the wide quantum well subband energy levels. The asymmetric double quantum well configuration

has a relatively stable conduction subband energy state in a narrow quantum well and an unstable state in a wide active quantum well, with band mixing or tunneling providing the instability.

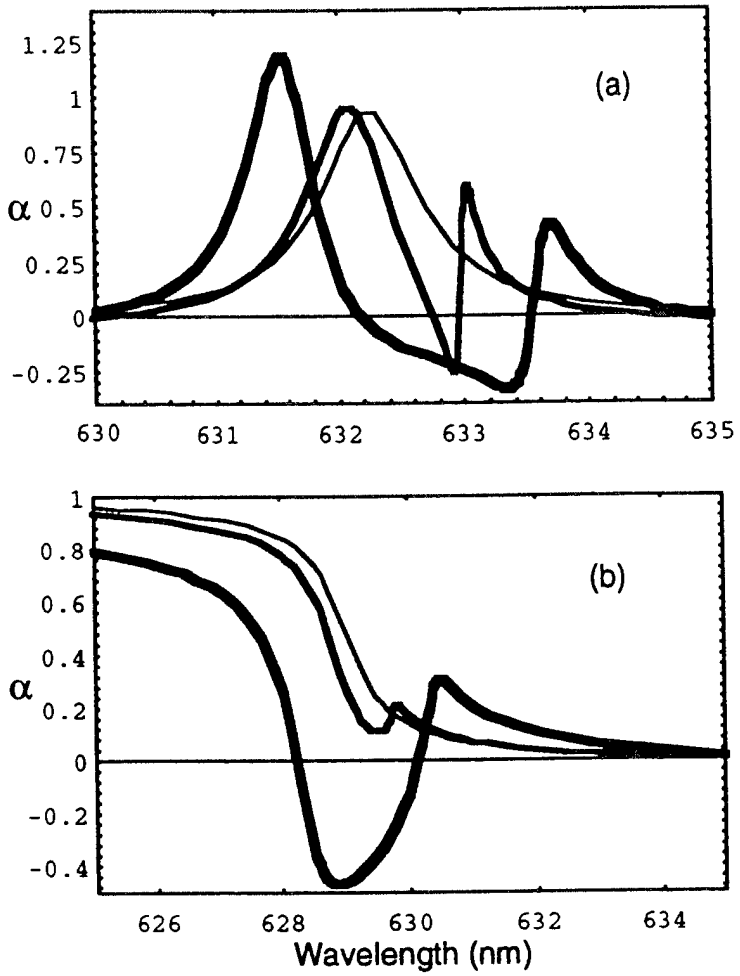

Figure 4.4 Absorption profile in the intrinsically coupled asymmetric double quantum well.
(a) Excitonic transition for gain without population inversion.
(b) Continuum transition for gain without population inversion.

The optical properties of the intrinsically coupled asymmetric double quantum well are comparable with the electromagnetically coupled asymmetric quantum structure except for off-resonant coupling. In principle, it is possible to exactly match energy levels from two different size quantum well, resulting in resonant intrinsic coupling (equivalent to zero frequency optical coupling). Practically speaking, however, such an accidental degeneracy will be difficult to achieve and off-resonant coupling will occur. If the system is too far off-resonance, it will not exhibit zero absorption or gain without population inversion. Figure 4.4 depicts the off-resonant results for realistic gain without inversion. Zero absorption is also possible.

Figure 4.4.(a) shows the excitonic gain without population inversion. Since the carrier injection rate can be easily controlled in the intrinsic configuration, ***excitonic microlasers*** *are a possibility we will investigate.*

For continuum transitions, Fig. 4.4.(b) shows gain without population inversion for moderate coupling strength. Therefore, thresholdless ***laser diode as lasing without inversion*** *are possibilities we will investigate.*

Figure 4.4 describes the gain profiles as function of coupling strength from 0 meV to 3 meV. Most intrinsic couplings are much larger for reasonable coupling barrier thicknesses within the tunneling coherence length. Therefore, we anticipate intrinsic coupling to remain in existence when the structure is placed under an external electric field.

In contrast to interband transitions, intersubband transitions have already demonstrated lasing under inversion at low temperature using the lifetime determining mechanisms we've mentioned [Faist et al. 1994]. For lasing without inversion, a similar unipolar device was recently proposed using an asymmetric double quantum well wherein tunneling controls the lifetime [Imamoglu & Ram 1994]. Since intrinsic coupling does not require external optical fields, modulation of intersubband transitions using the zero absorption or gain without inversion mechanisms occur. The configuration can be built by adding one more stable ground state in the wide quantum well region to replace the valence subband ground state.

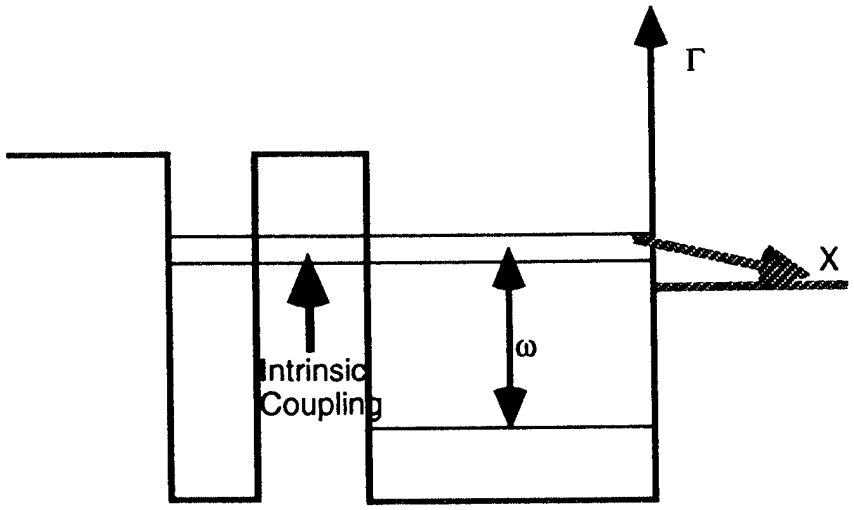

Figure 4.5 Intrinsically coupled asymmetric double quantum well configuration with a band mixing decay path makes zero absorption and gain without inversion for intersubband transitions via quantum interference on the conduction band.

Figure 4.5 shows an intrinsically coupled system for intersubband transitions utilizing a band mixing-induced scattering decay path. The configuration consists of a $Al_{0.5}Ga_{0.5}As$ barrier, two quantum wells of 2.5 nm and 8 nm of $Al_{0.2}Ga_{0.8}As$ layers with a 5.5 nm $Al_{0.5}Ga_{0.5}As$ coupling barrier, and a AlAs band mixing barrier layer. This quantum well system has no continuum absorption problem, as the subband dispersion relations are parallel parabolic around the $k=0$ band edge momentum. Since the intersubband transition uses only conduction electrons, we refer to this as a unipolar device.

The intersubband transition usually occurs around the band edge at momentum $k=0$, and it has characteristics similar to atomic transitions because of the parallel subband structure. In particular, the carrier population distribution depends on the Fermi function with energy given by $E_z + \hbar^2(K_x + K_y)/2m^*$. Summation must occur over the occupied parallel intersubband transitions. In addition, intersubband dipole matrix elements are larger than the interband elements by roughly the ratio of the well width to the unit cell dimension, drastically increasing the overall transition results. Therefore, our modeling shown in Fig. 4.6 results in better contrast than intrinsically coupled interband transition, and nearly atomic transition profile shapes. Figure 4.6 shows the same shape as the excitonic interband transition of Fig. 4.4.(a), but zero absorption and gain without inversion occur at lower coupling fields. In the figure, off-resonant coupling introduces the asymmetric absorption profiles.

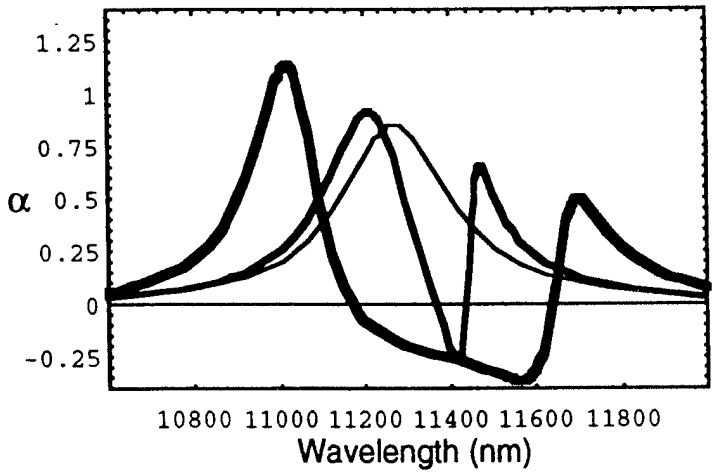

Figure 4.6 Absorption profile of intrinsically coupled intersubband transitions in an asymmetric double quantum well shows gain without population inversion. Coupling strength varies form 0 meV to 3 meV

From intersubband transitions using intrinsic coupling, we can investigate construction of unipolar long IR microlaser diodes at room temperature.

4.3 Applications of Gain without Inversion Mechanism

We have proposed several gain without inversion configurations and discussed their basic applications. This section shows more details of the representative applications. The primary concerns are gain factors, index changes, and population distributions. The following section examines optical modulators and compensators, optical amplifiers and lasing without inversion, excitonic laser diodes as a thresholdless microlaser, and nonlinear generation mechanisms. For our calculations, we assume equal electron and hole injection. In addition, for excitonic transitions, we have used our density matrix result assuming a delta function-like density of states. One goal of our planned program is to improve upon our essentially single electron models by incorporating many body effects.

4.3.1 Optical Modulators and Group Velocity Compensators

All zero absorption configurations exhibit large absorption modulation and hence gain without population inversion under small excited state populations. Since zero absorption is the first step to make gain without inversion, zero absorption modulation is a possible near term device application. For electromagnetic intersubband coupling, the modulation of absorption occurs as fast as the intersubband sub-picosecond carrier relaxation time. Unlike the interband modulation mechanism, the modulation arises from the intersubband coupling and does not depend on either transitions into a ground state or saturation effects. Figure 4.7.(a) depicts the modulation of excitonic absorption by intersubband coupling in the asymmetric quantum well of Fig. 4.1. The figure shows an ideal on-off ratio if the zero absorption condition exists.

Since the zero absorption window is very narrow, the corresponding index change also results in a large index modulation at the resonant frequency as shown in Fig. 4.7.(b). The index change can have group velocity compensation applications adjustable by coupling strength. Since the figure present normalized values of absorption and index change for the zero coupling case, the actual modal absorption and index change for a prototype edge waveguide are close to 735/cm and ±0.07, respectively. Increasing the confinement factor in MQW structures with a short active length can result in absorption and index modulations of 10000/cm and 0.9 respectively.

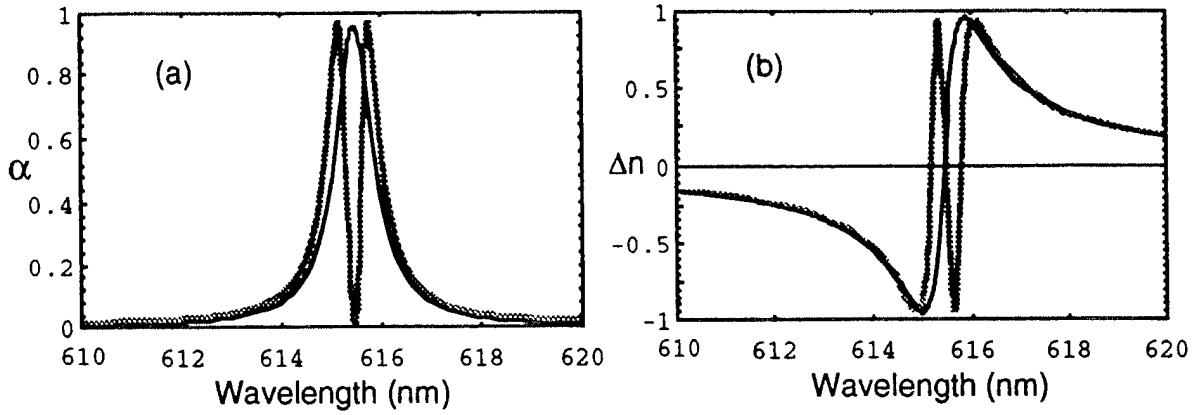

Figure 4.7 Electromagnetically coupled asymmetric quantum well shows functionality of excitonic transitions for coupling strengths, 0 meV to 1 meV as solid to gray line.
(a) Zero absorption modulation with sub-pico second response.
(b) Adjustable index changes introduces group velocity compensation.

Excitonic absorption modulation is useful for weak signal, but is expected to exhibit saturation effects in the presence of strong signals. To increase modulation, an excited carrier population can be introduced.

4.3.2 Optical Amplifiers and Lasing without Inversion

The intrinsically coupled system theoretically exhibits gain without population, and therefore can amplify photon signals or show lasing without population inversion. The configuration without excited carrier shows zero absorption at 632.8 nm with asymmetric side band absorption profiles that comes from off-resonant coupling. With excited carriers, it shows gain without population inversion as shown in Fig. 4.8.(a). The origin of the gain differs from a two level system, so gain without inversion profile always has a pre-absorption peak that originates from Rabi splitting. The value of the material gain is comparable, in the range of 450/cm to 1320/cm, with normal edge emitting laser diode structures for reasonable coupling and pumping.

For optical amplification, we need gain without inversion, and all our configurations are useful. To amplify signal without feedback, edge emitting laser diode structures with angle incident is suitable. Unlike normal two-level systems, however, gain without population inversion has the different index modulation effect as shown in Fig. 4.8.(b). The difference of index change is about 0.1. ***The noise and nonlinearities as characterized by the linewidth enhancement factor are planned to be investigated for this novel amplification mechanism.***

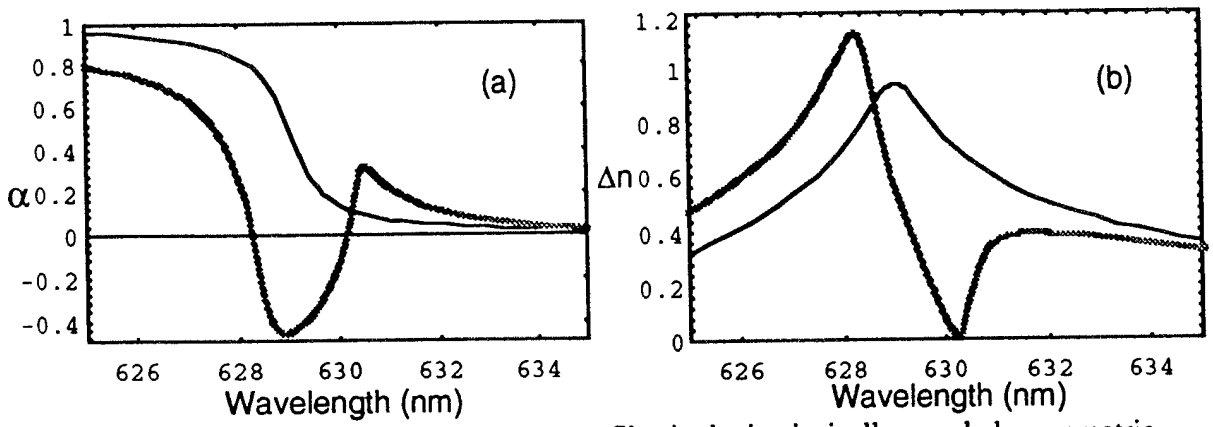

Figure 4.8 Absorption and index change profiles in the intrinsically coupled asymmetric double quantum well for coupling strength 0 meV and 3 meV.
(a) Continuum transition for gain without population inversion.
(b) Index change profiles for continuum transitions.

For lasing without inversion, we need to add a cavity and the proper waveguiding. Since the configuration has large material (bulk) gain, a VCSEL or edge emitting laser can be used to demonstrate lasing without inversion. To achieve the above gain, however, the quasi Fermi energy for the conduction band is above the n=1 subband energy level but below the n=2 (where lasing takes place). It means that there is still a strong threshold condition, but much lower than the threshold for lasing on the n=2 transition. However, in this configuration, n=1 and n=2 are closely spaced. The main challenge for intrinsic coupling is the maintaining the coupling during DC or optical current injection. Long IR intersubband transitions might prove a productive path as well.

This configuration has a narrow gain profile resulting in a narrow spontaneous emission line width and less spontaneous emission noise. For excitonic transitions the window is even narrower. Together with gain without inversion, an excitonic microlaser without a high Q cavity would be considerably different than the recently reported atomic microlaser [An et al. 1994].

4.3.3 Excitonic Laser and Microlasers

Laser diodes have been around for a long time and the threshold has been significantly reduced. Since continuum transitions result in broadened gain profiles, it is extremely difficult to build a single carrier laser at near-visible wavelengths. Our suggested solution is to use excitonic lasing without population inversion, relying on others to develop superhigh Q microcavity approaches and instead, concentrating on thresholdless gain media. So far only the microcavity approaches have been successfully applied to low threshold laser diodes.

The zero absorption configuration for gain without inversion together with a microcavity is our proposed excitonic microlaser diode. We plan to use the intrinsically coupled asymmetric double quantum well for gain without inversion, with a VCSEL cavity. Figure 4.9 describes excitonic transitions under inversionless conditions. With proper injection, the quasi Fermi energies are below the active conduction and valence subband energy levels. The relative populations are 0.94 for the n=1 valence subband electrons, 0.5 for the n=1 and 0.1 for n=2 conduction subband electrons, respectively. Our estimation of relative material gain in Fig. 4.9.(a) is 1880 cm^{-1}. Figure 4.9.(b) reveals the large index change, 0.12 to 1.6, arising from resonant excitonic peak. The main issues for excitonic lasing are the effect of this large index on the optical cavity and injection levels necessary to conserve excitonic transitions during gain without population inversion. Unlike conventional microcavity lasers, however, our microlaser does not require a high Q cavity, and any excited carrier around band edge energy is exposed to the competing processes of gain and screening.

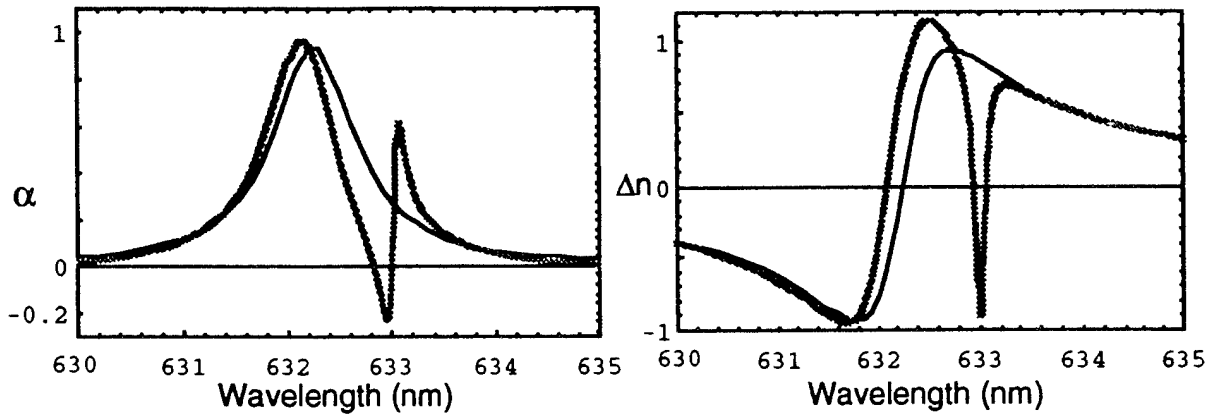

Figure 4.9 Excitonic absorption and index change in intrinsically coupled asymmetric double quantum well for coupling strength 0 meV and 1 meV.
(a) Excitonic transition shows gain without population inversion.
(b) Index change profiles for the corresponding excitonic transition.

5. TECHNICAL APPROACH

We have described the proposed electromagnetic and intrinsic coupling mechanisms in the last chapter. We now describe the total approach for real experiments. First growth and characterization of optimized sample designs are discussed, then the details of sample preparation and the experiments are considered.

5.1 Sample Design

Zero absorption and gain without inversion schemes have been treated for single quantum wells. To enhance signals, we need add more quantum wells, and confine the optical fields using waveguides or cavities. VCSEL structures can be used for the excitonic microlaser, and edge emitting structures for general studies of lasing without inversion or optical amplifiers. Detailed sample designs, will be based on our well developed device modeling programs, which include all absorption and index changes, subband energy level calculations, and determination of the optical fileds in a cavity.

5.1.1 Multiple Quantum Well Structures

Multiple quantum well structures are one of the easiest way to enhance single quantum well effects when the optical phase is not an important consideration. For example, optical modulators, group velocity compensators, and optical amplifiers are not as sensitive to optical phase as laser oscillations or nonlinear processes. We plan to use undoped MQW structures for all configurations to investigate the basic possibility of zero absorption toward gain without population inversion. We consider the applications of a simple multiquantum well system.

For optical modulation, the excitonic absorption coefficient (without coupling) is close to 10000 cm^{-1} or 1 μm^{-1} over a well width of 5 to 10 nm. Without enhancement therefore, a transmission modulator requires at least 100 quantum wells to reach a e^{-1} modulation ratio. The total thickness of MQW structure could be 5 to 6 μm. If we adopt an asymmetric F.-P cavity structure, we can double the modulation effect using the backside reflectiion, reducing the sample thickness by half. Since the front surface of AlGaAs has about 30% reflection without an AR coating and the bottom mirror has 99% reflectivity, the total structure behaves as a 5 μm thick asymmetric F.P. cavity. The cavity length can be adjusted controlling a spacing layer using wet etching. To enhance input coupling, the top layers of active region can be AR coated, reducing the asymmetry of the cavity. Coupling will modulate the absorption and refractive index with a sub-pico second response limited by the intersubband carrier lifetime.

Since group velocity modulation depends on the refractive index change, group velocity compensators use the same structures as optical modulators. The main application of group velocity compensation is in pulse shaping and different pulse shapes require different index dispersions. This is controlled by coupling strength. For pulse compression or generation, the rapid index change associated with the absorption dip can be helpful. In addition, the

compensator does not require a fast response, and can use the intrinsic coupling mechanism.

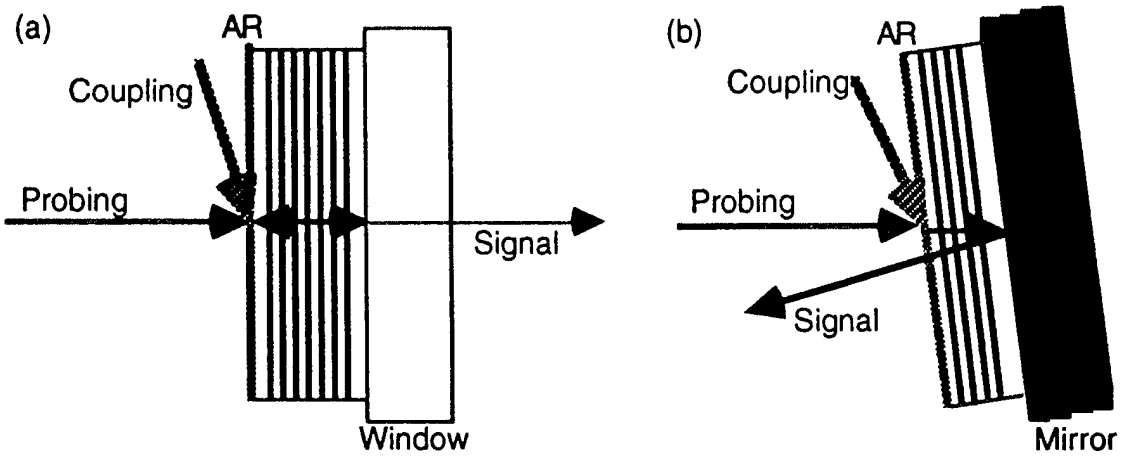

Figure 5.1 Optical modulators and group velocity compensator with asymmetric quantum structures, where the coupling arrows represent intersubband coupling laser as modulation source or intrinsic coupling of group velocity compensators.
(a) Transmission configuration with 100 asymmetric quantum wells.
(b) Reflective configuration with 60 asymmetric quantum wells.

Figure 5.1 describes both modulators and group velocity compensators with active layers placed on a window or a mirror. To separate active layers from substrates requires a technique described later. In the figure, the optical coupling field is incident at the Brewster angle for nearly 100 % coupling efficiency. For example, a CO_2 laser will be efficiently coupled into AlGaAs multilayer thin films at 72^o given the proper polarization.

Multiquantum well structures can also be used for nonlinear generation. Surface normal nonlinear generation using counterpropagating fundamental fields are simple structures for demonstraing nonlinear properties without concern for phase matching conditions. Our group has studied second harmonic generation using quasi phase matching in AlGaAs multilayer structures [Zou 1994]. However large absorption above band edge results in very low efficiency. If we use our asymmetric quantum structures, we can remove propagation loss using zero absorption or gain without inversion. Figure 5.2 depicts the quasi phase matching structures with our zero absorption configuration using electromagnetically coupled asymmetric quantum well of Fig. 4.10. Figure 5.2.(a) describes two counterpropagating fundamental fields and generated second harmonics, the counter propagating field can be produced as the reflected field from a facet of the sample. However, we may need to make wave guiding structure by some sample preparation. Figure 5.2.(b) magnify the part of active layers in the wave guiding structure. Multi quantum well structure can have as many layers as possible to be grown if phases of nonlinear generations are constructive. Therefore the polarity of asymmetric quantum wells are changed to alter the sign of phase at every half wavelength.

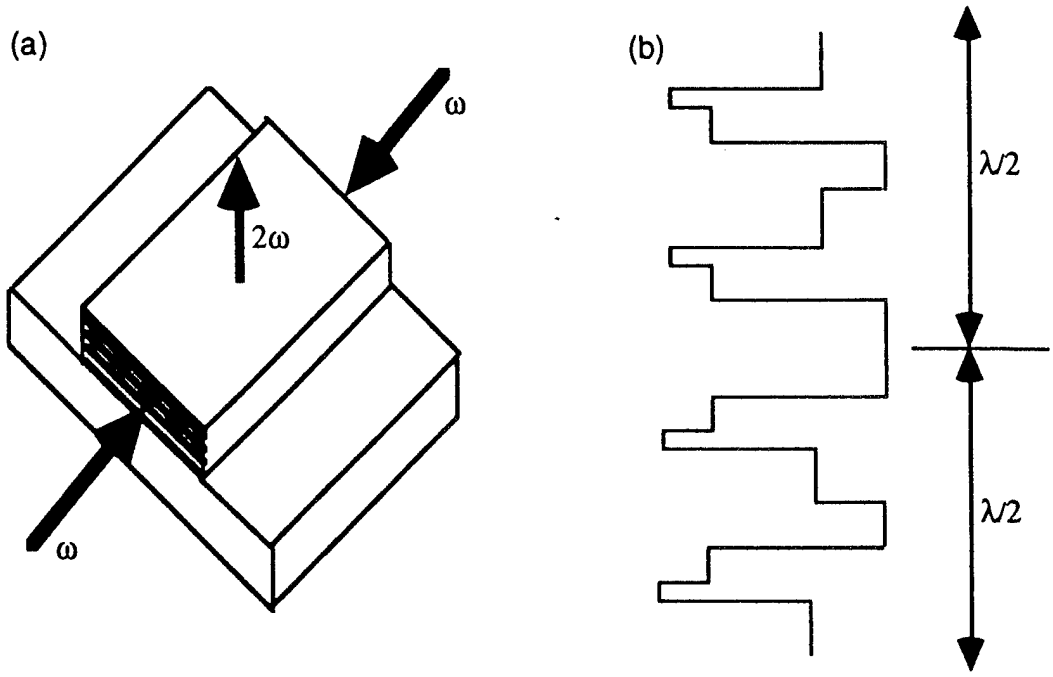

Figure 5.2 Nonlinear generation scheme with asymmetric quantum wells uses a quasi phase matching by alternative combination of asymmetric quantum wells at every λ/2.
(a) Waveguiding structure for surface normal second harmonic generation.
(b) Quasi phase matching as a part of active layers on conduction band edge.

5.1.2 Edge Emitting and Surface emitting Cavity Structures

Cavity structures in semiconductors are categorized as either edge emitting or surface emitting cavities. While edge emitting cavity structures have very long cavity lengths (100μm to 1 mm) that can be as long as necessary to amplify signals, they have limited confinement factors. For surface emitting cavity structures, the cavity lengths are limited multiple of half wavelength of signals, but the confinements is more effective. Undoped samples using optical pumping are the first step in test our investigations, but both cavity structures will be used for investigating electrical injection in the intrinsically coupled configuration.

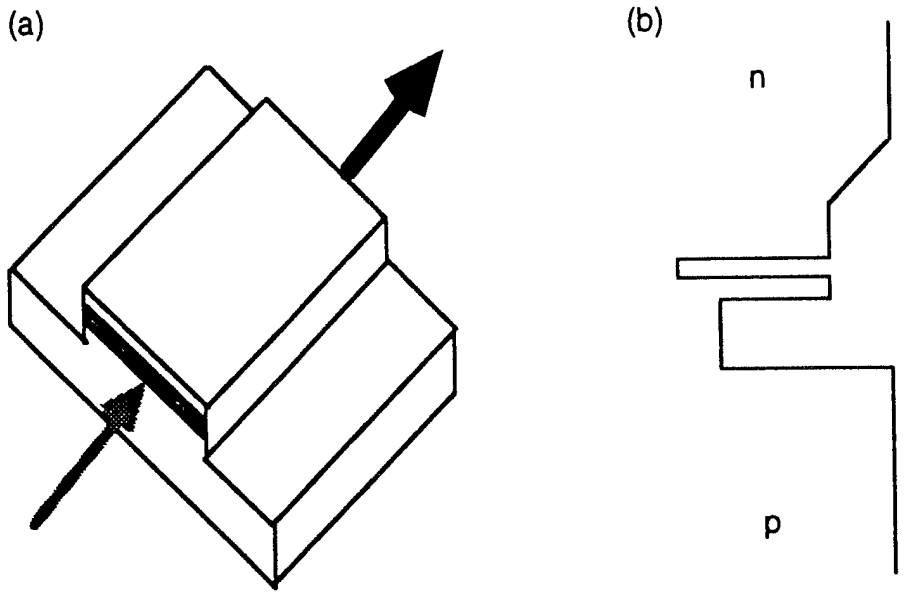

Figure 5.3 Edge emitting cavity with the asymmetric quantum well for a optical amplifier and a laser diode as lasing without inversion.
(a) Waveguiding structure for edge emitting cavity.
(b) Electrical polarity of active layers on conduction band edge.

Our gain without inversion configurations simply replace the active layers of standard optical amplifiers and laser diodes. Then we investigate threshold reductions. In a standard optical amplifier or laser diode, the active region is replaced by our asymmetric double quantum well. Figure 5.3.(a) shows a brief sketch.

Microcavity laser diodes have been developed for ultra low threshold laser or thresholdless laser diode using a surface emitting cavity structure. So far a one atom microlaser has been demonstrated [An et al. 1994], but vertical cavity surface emitting structures in semiconductors have not shown such behavior even at low temperature. We propose to use gain without inversion for microlasers using a possible excitonic lasing scheme.

Since a microlaser is characterized by thresholdless lasing, an excitonic laser diode using gain without population inversion is a good candidate. Normal electrical injection requires population inversion, with no surviving excitonic transitions. However, gain without population inversion makes any amount of excited carriers contribute gain. All we need is the addition of microcavity to recover internal loss. Since gain does not require population inversion, a high Q microcavity is not necessary. Instead, a normal VCSEL (high Q in only one dimension) may be good enough. Figure 5.4 describes our proposed microlaser structure for the study of possible excitonic lasing at room temperature. To construct the microcavity of Fig. 5.4.(a), the first step is

to remove the substrate after p-type metallization, then finish processing with the n-type contact and dielectric DBRs.

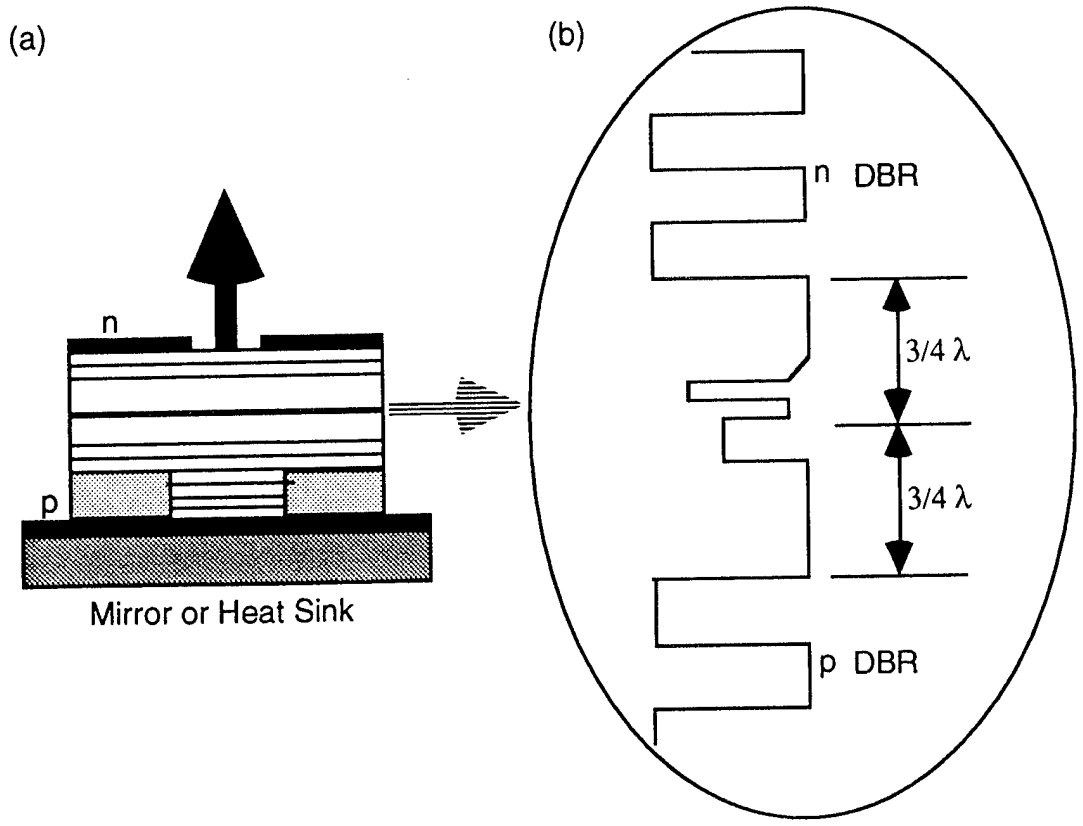

Figure 5.4 Surface emitting cavity with the asymmetric quantum well for excitonic lasing as a microlaser diode with lasing without inversion.
(a) Microcavity structure of vertical cavity surface emitting laser.
(b) VCSEL structure of active layers on conduction band edge.

5.2 Sample Growth and Characterization

Our center has 2 MOCVD and 1 MBE systems in the crystal growth facility. Since the crystal growth facility has specializes for laser diode, we have grown successfully various DFB-RPG, VCSEL, and edge emitting laser diodes. We anticipate using the MBE for the undoped samples (electromagnetically coupled configurations) and MOCVD or MBE for doped samples (intrinsically coupled configurations).

After growth samples are characterized by, PL, PLE, and PR to determine subband energy levels, and reflectivity and transmission measurements gives excitonic properties. Normal reflectivity measurements analyze sample thicknesses and cavity qualities. For electrical characterization, we can use our DLTS, I-V, and C-V measurements to reveal defect levels and

impurity density and other electrical parameters. In addition, SEM, TEM, X-ray diffraction, Hall effect, and so on will be used for material characterization.

5.3 Sample Preparation

Once a is sample grown, it needs to be prepared for experiments. In the center, class 100 clean room provide all necessary equipment. For most optical measurements, removing the GaAs substrate is necessary using lapping and jet etching or HF etching and Van der Waals bonding. These techniques of removing substrates can be used for all applications and configurations, including those that require further processing such as ohmic contact, wire bonding or dielectric coating.

5.4 Steady State Experiment

We have solved the steady state density matrix equation in the frequency domain and thus far our experimental set-up mimics the time independent CW regime. To study carrier dynamics, we can add time resolved techniques. All experimental set-ups are straightforward to perform at either room tempertture or liquid helium..

To study zero absorption and gain without inversion, the following experimental configuration can be used for both electromagnetically and intrisically coupled configurations. Figure 5.5. shows the zero absorption measurement setup.

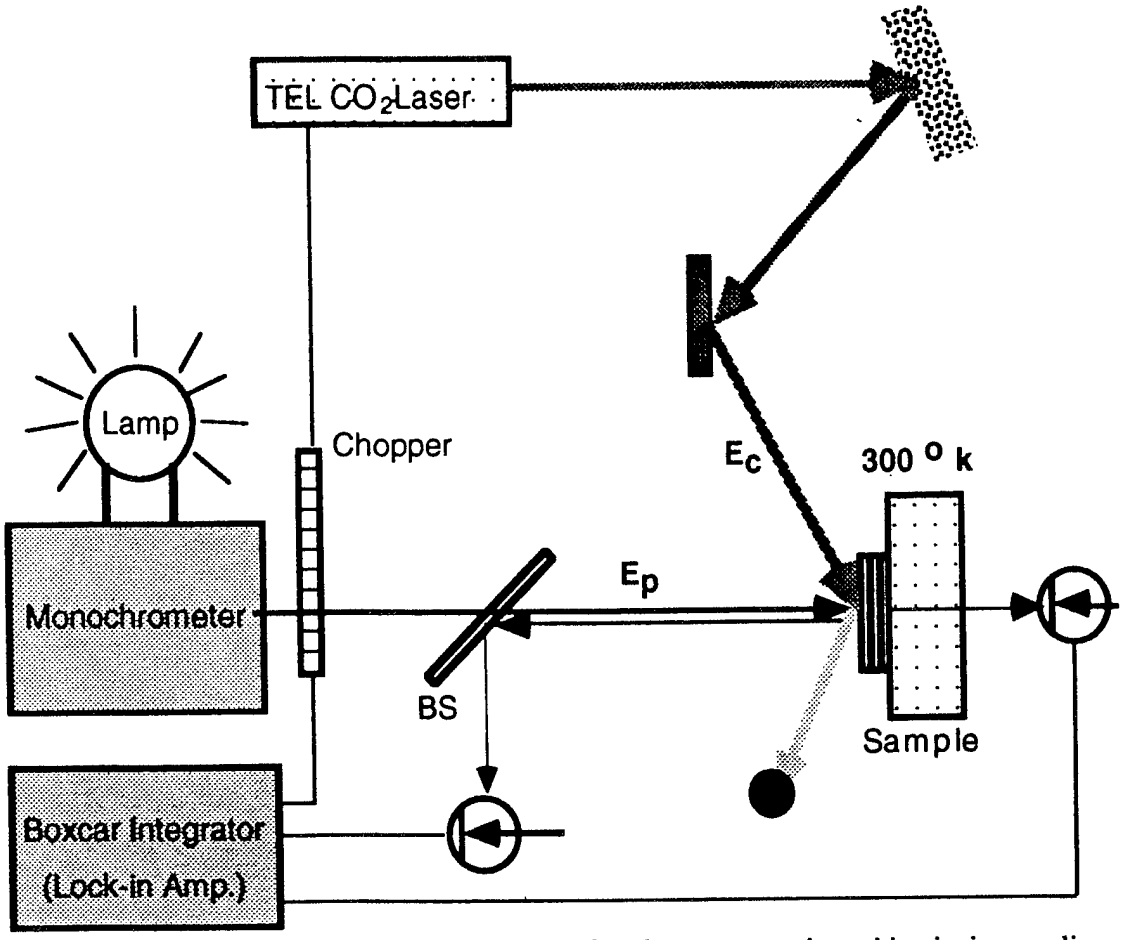

Figure 5.5 Zero absorption experimental setup for electromagnetic and intrinsic couplings.

In intrinsic coupling, the experiment setup is identical as a simple absorption measurement, so instead of a boxcar integrator, we can use a lock-in amplifier. However, for optical coupling, the synchronization between coupling and probing is necessary by a boxcar integrator. Figure 5.6 depicts details of optical coupling and signal detecting setup, where Fig. 5.6.(b) especially shows the gate window as a controller of intersubband coupling strengths.

For absorption modulation and group velocity compensation, time resolving system should be added. Then we can study carrier response and pulse shape modulation. If probing is replaced by the tunable solid state laser, Ti:Al_2O_3, without the limit of modulation source wavelength (10.6 μm), probing laser input and modulated signal recover the time dependent signal with a proper pulse picking system and a modified short coupling pulse. Since we already have a tunable solid state laser, we need to make a pulse picker to match with the CO_2 laser low frequency and use a special plasma switching technique to compress the CO_2 laser pulse. Therefore this time resolving setup is very complicated and challenging. However, intrinsic

coupling makes direct time resolving measurement possible by adding an interference measurement system.

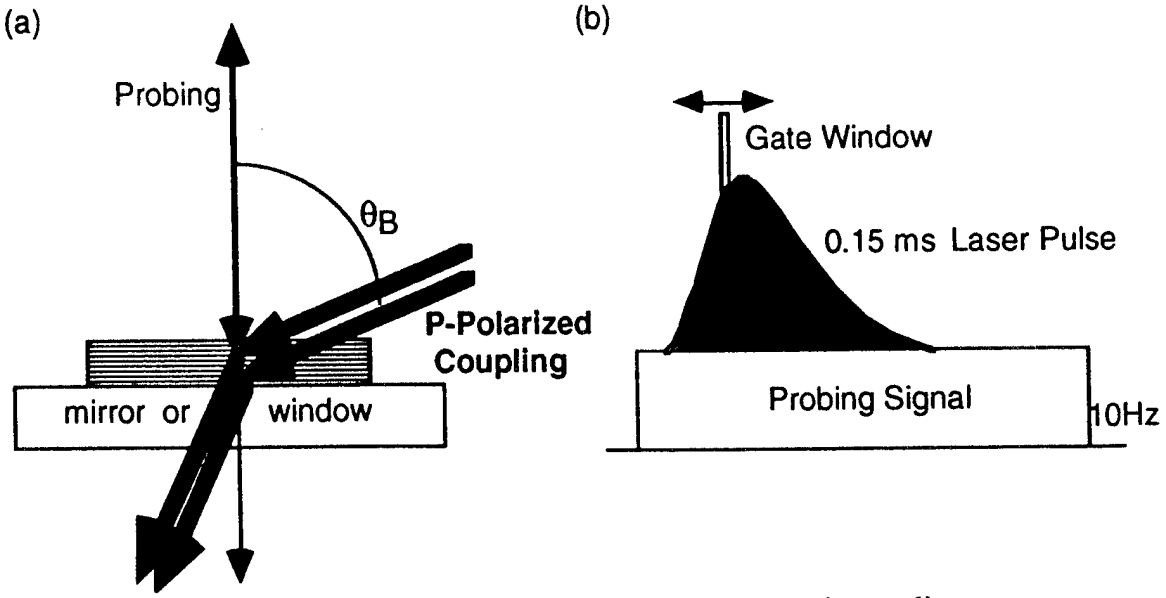

Figure 5.6 Zero absorption experimental detail for electromagnetic couplings.
(a) Intersubband coupling laser is incident at the Brewster angle.
(b) Gating and synchronization of probing and coupling.

If zero absorption is possible, the next step is to test whether to get gain without population inversion or not. So edge emitting optical amplifiers need to be tested for gain without inversion, which has the simple setup, then electrical or optical pumping mechanism is applied for lasing without inversion. Unlike optical amplifiers, lasing without inversion requires a sensitive detection system including spectrum analyzers and photon counting for the microlaser. In the long IR lasing mechanism of intersubband transitions, the experiment setup needs an IR detection system.

Figure 5.7 describes the general emission measurement system for electrical injection, which is easily converted for optical injection as well. Exact numbers and injected carriers for each energy levels must be monitored.

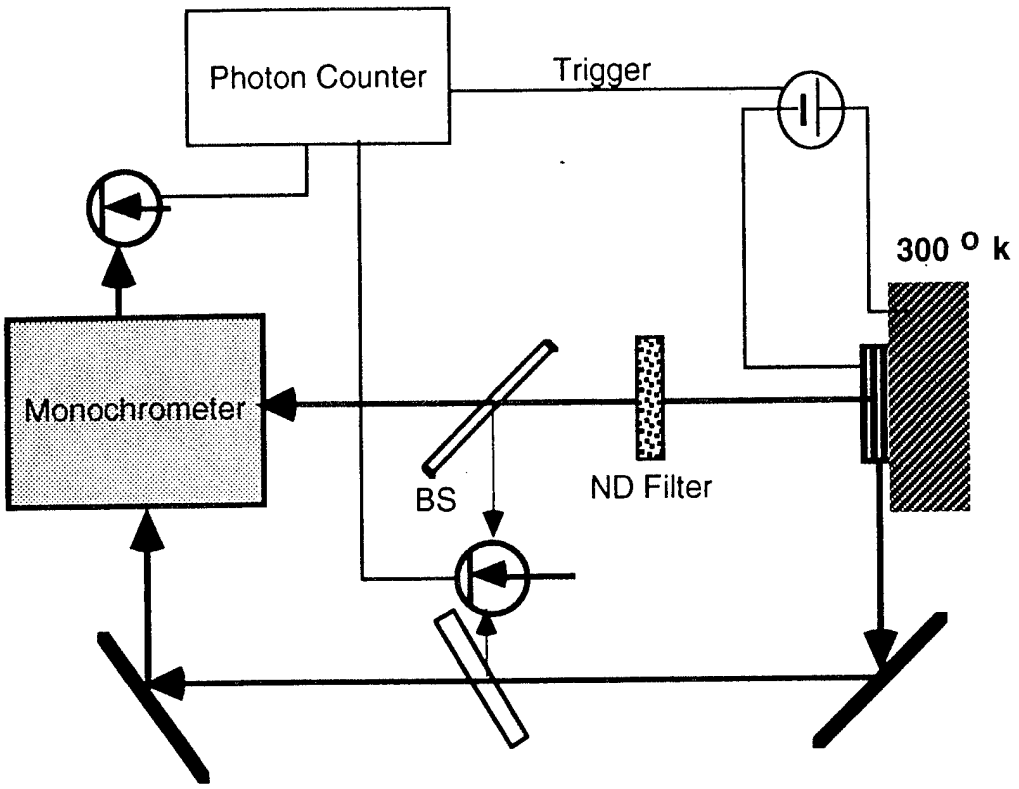

Figure 5.7 Lasing without inversion measurement setup for intrinsic coupling.

6. STATEMENT OF WORK AND TECHNICAL OBJECTIVES

Webriefly summarize our objectives. We will investigate theoretically and experimentally zero absorption with applications toward optical amplification, gain without population inversion, and lasing without inversion in asymmetric quantum wells. Our final goal is to demonstrate an excitonic microlaser, lasing without population inversion using the intrinsically coupled configuration and electrical carrier injection.

6.1 Improvement of Theory and Modeling

7.1.1 Homogeneous and inhomogeneous broadening effects for MQW structures.
7.1.2 Improvement of momentum space integration in the total simulation.
7.1.3 Time dependent population distributions for DC and short pulse operation.
7.1.4 Cavity dynamics for population distributions as a function of injection.
7.1.5 Cavity modeling under high intensity optical fields.
7.1.6 Linewidth and noise reduction measurements and theory.
7.1.7 Excitonic coupling mechanism theory.
7.1.8 Inclusion of many-body effects in formalism.

6.2 Sample Design, Growth, and Characterization

7.2.1 General MQW sample design using asymmetric quantum wells
7.2.2 Edge emitting cavity design with dual waveguiding structures.
7.2.3 Vertical cavity design with dielectric or metal mirrors.
7.2.4 Design of spacing layers in terms of electrical pumping.
7.2.5 Growth of microlaser structures.
7.2.6 Calibration and characterization for doping level and energy levels .

6.3 Sample Preparation and Experiment

7.3.1 MQW samples using Van der Waals bonding.
7.3.2 Experiments on zero absorption modulation and gain without population inversion.
7.3.3 Microcavity process development with special etching techniques.
7.3.4 Experiments on microlasers based on lasing without inversion.

7 QUALIFICATIONS OF PERSONNEL

KEVIN J. MALLOY

EDUCATION

Stanford University
Ph.D., January 1984 under G. L. Pearson
Electrical Engineering

University of Notre Dame
B.S., May, 1978
Electrical Engineering

EXPERIENCE

January 1990 to Present — **ASSOCIATE (SINCE JUNE 1994)) PROFESSOR OF ELECTRICAL AND COMPUTER ENGINEERING, THE UNIVERSITY OF NEW MEXICO.** Member of the Center for High Technology Materials. I teach and conduct research on optoelectronic devices and materials.

November 1988 to January 1990 — **VISITING ASSOCIATE RESEARCH ENGINEER, THE UNIVERSITY OF CALIFORNIA - BERKELEY.** Worked with Professors Shyh Wang and Eicke Weber on semiconductor lasers and defects.

October 1983 to October 1988 — **USAF CAPTAIN AND PROGRAM MANAGER FOR ELECTRONIC MATERIALS, THE AIR FORCE OFFICE OF SCIENTIFIC RESEARCH, WASHINGTON, DC.** Responsible for implementing and managing $6 million in basic research funding and coordinating Air Force-wide research.

May 1978 to September 1978 — **ELECTRONIC TECHNICIAN, AIR FORCE AVIONICS LABORATORY.** Brought one of the nation's first MBE machines on line

HONORS

•Air Force Commendation Medal for participation in Project Forecast II
•Air Force Meritorious Service Medal for exceptional service.

•UNM School of Engineering Researcher of the Year Award

PROFESSIONAL ACTIVITIES

•Member of the IEEE, MRS, AVS and APS
•Advisory Board for Critical Reviews in Solid State and Materials Science.
•Advisory Committee for International Conference on Hot Carriers in Semiconductors and the Conference on the Physics and Chemistry of Semiconductor Interfaces.

PUBLICATIONS

* Indicates UNM Student

1. K. J. Malloy and C. L. Giles, "Implementation of Neural Networks: Optical Architectures and Devices," *Materials Research Society Proceedings,* **109** edited by D. Ulrich, 1988, Pittsburgh, PA.

2. K. J. Malloy and J. A. Van Vechten, "Temperature dependence of the HgTe-CdTe band offset," *Appl. Phys. Lett.* **54**, 937 (1989).

3. J. A. Van Vechten and K. J. Malloy, "The temperature dependence of band offsets for semiconductor heterojunctions," *J. Phys: Condens. Matter* **2**, 281 (1990).

4. J.-P. Weber, K. J. Malloy and S. Wang, "Effects of layer thickness variations on vertical cavity surface emitting DBR semiconductor lasers," *Photon. Technol. Lett.* **2**, 162 (1990).

5. W. Hsin, G. Du, J. K. Gamelin, K. J. Malloy, S. Wang, J. R. Whinnery, Y. J. Yang, T. G. Dziura, and S. C. Wang, "Low threshold DBR surface emitting laser diode with semiconductor air-bridge supported top mirror," *Electronics Lett.* **26**, 307, (1990).

6. J. D. Walker, K. J. Malloy, S. Wang And J. S. Smith, "Precision AlGaAs Bragg reflectors fabricated by phased-locked epitaxy," *Appl. Phys Lett.* **56**, 2493 (1990).

7. P. Harshman, K. J. Malloy, and S. Wang, "The role of Aluminum in MBE growth of (111B) GaAs," "Materials Research Society Proceedings," **198** edited by D.W. Shaw, et al., 1990, Pittsburgh, PA.

8. H. P. Lee, X. Liu, K. J. Malloy, S. Wang, T. George, E. R. Weber, and Z. Lillienthal-Weber, "Structural Characteristics and Initial Nucleation of GaAs on Si Films Grown by Modulated Molecular Beam Epitaxy," *J. Electron. Materials*, **20**, 179 (1991).

9. C. F. Schaus, A. J. Torres, J. Cheng, S. Sun, C. Hains, K. J. Malloy, H. E. Schaus, E. A. Armour, And K. Zheng, "Transverse junction vertical-cavity surface- emitting laser," *Appl. Phys. Lett.* **58**, 1 (1991).

10. K. J. Malloy and J. A. Van Vechten, "Thermal Expansion Contributions to Band Gap and Offset Temperature Dependences" *J. Vacuum Science and Technol.* **B9** 2212 (1991).

11. D. L. Kendall, C. B. Fledderman and K. J. Malloy, "Critical Technologies for the Micromachining of Silicon," book chapter in Semiconductors and Semimetals: The Mechanical Properties of Semiconductors (Vol. 37) K Faber and K.J. Malloy, Eds. (Academic Press, Boston, 1992)

12. K. J. Malloy and K. Khachaturyan, "DX and Related Defects in Compound Semiconductors," book chapter in Semiconductors and Semimetals: Defects in Compound Semiconductors (Vol. 38), E. Weber, Ed. (Academic Press, Boston, 1992).

13. G. Guel*, E. A. Armour, S. Z. Sun, S. T. Srinivasan, K. J. Malloy and S. D. Hersee, "Reduction of deep levels in MOCVD-regrown $Al_xGa_{1-x}As$ interfaces by $(NH_4)_2S$ passivation and in-situ HCl etching," *J. Electron. Mater.* **21** 1051 (1992).

14. J. A. Lott*, R. P. Schneider, Jr., G. A. Vawter, J. C. Zolper, and K. J. Malloy, "Visible (660nm) resonant cavity light emitting diodes," *Electronics Letters,* **29** 328 (1993).

15. J. A. Lott*, R. P. Schneider, Jr., J. C. Zolper, and K. J. Malloy, "AlGaInP visible resonant cavity light-emitting diodes," *Photon. Technol. Lett.*, **5** 631 (1993).

16. J. L. Reno, S. Chadda*, and K. J. Malloy, "Dislocation density reduction in CdZnTe(100) on GaAs by using strained layer superlattices," *Appl. Phys. Lett.*, **63** 1827 (1993).

17. J. A. Lott*, R. P. Schneider, Jr., J. C. Zolper, and K. J. Malloy, "AlGaInP visible vertical cavity surface emitting lasers operating with gain contributions from the n=2 quantum well transition," *Appl. Phys. Lett.*, **63** 3485 (1993).

18. R. P Schneider, Jr., J. A. Lott*, K. D. Choquette, J. J. Figiel, S. A. Samora and K. J. Malloy, "Efficient room temperature continuous-wave operation of AlGaInP/AlGaAs vertical-cavity surface emitting laser diodes," *Photon. Technol. Lett.*, **6** (1994).

19. D. S. Lee* and K. J. Malloy, "Analysis of reduced interband absorption mechanisms in semiconductor quantum wells," *IEEE J. Quantum Electron.*, **30** 85 (1994).

20. E. R. Brown, K. Agi*, C. D. Dill III, C.D. Parker, and K. J. Malloy, "A new face-centered-cubic photonic crystal for microwave and millimeter wave applications," *Microwave and Opt. Tech. Lett*, **7**, 777 (1994).

21. J. A. Lott*, R. P. Schneider, K. J. Malloy, S. P. Kilcoyne, and K. D. Choquette, "Partial Top Dielectric Stack Distributed Bragg Reflectors for Red Vertical Cavity Surface Emitting Laser Arrays," *Photon. Technol. Lett.*, **6** 1397 (1994).

22. K. Agi*, E. R. Brown, C. D. Dill III, O. B. McMahon, and K. J. Malloy, "Ultra-wideband photonic crystals for broadband antenna applications," *Electronics Lett*, to appear Jan 1995.

REVIEWED CONFERENCE PUBLICATIONS

* Indicates UNM Student

1. L. C. Lou* and K. J. Malloy, "Multilayer design for efficient waveguide surface normal second harmonic generation," *Conference on Lasers and Electro-Optics* (CLEO-92), Anaheim, CA, *1992 OSA Technical Digest Series* **12** 394 (1992).

2. T. Sze*, M. Mohbobzadeh, J. Cheng, S. Hersee, M. Osinski, S. R. J. Brueck and K. J. Malloy, "Profiling of MOCVD- and MBE-grown vertical cavity surface emitting laser wafers for wavelength division multiplexing sources," *SPIE '93*, Los Angeles, CA.

3. J. A. Lott*, R. P. Schneider, Jr., and K. J. Malloy, "Design, fabrication and performance of $In_y(Al_xGa_{1-x})_{1-y}P/Al_xGa_{1-x}As$ visible resonant cavity light emitting diodes," paper D1-5.5 at*Materials Research Society Spring Meeting*, San Francisco, CA, April 1993.

4. S. Chadda*, K. J. Malloy, and J. L. Reno, "Defect reduction in $Cd_{1-x}Zn_xTe$ epilayers on GaAs substrates," *Materials Research Society Symposium Proceedings*, **299**, 191 1994.

5. J. A. Lott*, R. P. Schneider, Jr., and K. J. Malloy, "All $In_y(Al_xGa_{1-x})_{1-y}P$ visible (672nm) vertical cavity surface emitting laser," paper CWJ56 at *CLEO '93*, Baltimore, MD, May 1993.

6. D. S. Lee* and K. J. Malloy, "Induced interband transparencies in semiconductor quantum wells," *QELS '93. Technical Digets*, 243 (1993).

7. L. C. Zou* and K. J. Malloy, "Measurement of the dispersion of the second order nonlinear susceptibilities of high aluminum component $Al_xGa_{1-x}As$," *OSA Technical Digest Series*, **12** 108 (1993).

8. J. A. Lott*, R. P. Schneider, Jr., and K. J. Malloy, "Electrically injected AlGaInP visible vertical cavity surface emitting laser operating at the n=2 quantum well transisiton," postdeadline paper CPD3 at *CLEO '93*, Baltimore, MD, May 1993.

9. J. A. Lott*, R. P. Schneider, Jr., and K. J. Malloy, "Visible (639<λ<661 nm) vertical cavity surface emitting laser diodes," paper IIIB-1 at *51st Annual Device Research Conference*, Santa Barbara, CA, June 1993.

10. J. A. Lott*, R. P. Schneider, Jr., J. C. Zolper, and K. J. Malloy, "Gain characteristics of red AlGaInP VCSELs," presented at *LEOS 93*, San Jose, CA, November 1993.

11. S. Chadda*, M. Pelcynski, S. Hersee and K. J. Malloy, "Structural evaluation of GaN grown on sapphire by MOCVD," to appear in *Materials Research Society Proceedings, Vol. xxx*, (Pittsburgh, PA, 1994).

12. K. Agi*, E. R. Brown, C. D. Dill, O. B. McMahon and K. J. Malloy, "An ultra-wideband photonic crystal," in *Ultra-Wideband, Short-Pulse Electromagnetics II*, (H. L. Bertoni, L. Carin, L. B. Felser, and S. V. Pillai, eds.), Plenum, New York.

13. D. S. Lee,* K. J. Malloy, O. Blum, and J. Klem "Observation of reduced interband absorption in semiconductor quantum wells," *CLEO/QELS '94. Late News Technical Digets*, 243 (1993).

14. Xinqiao Wang*, Hua Li, Carole Mourad*, J. G. McInerney and K. J. Malloy, "Reduction of linewidth enhancement factor in vertical cavity surface emitting lasers by temperature tuning," *CLEO-Europe Late News*, April 1994.

15. K. Agi*, E. R. Brown, O. B. McMahon, C. D. Dill, K. M. Molvar, and K. J. Malloy, "Characterization of a new face centered-cubic photonic crystal," to appear in *Guided Wave Optoelectronics: Device Characterization, Analysis and Design*, Plenum, New York.

8. FACILITIES AND EQUIPMENT

8.1 MOCVD & MBE Facility

CHTM's state-of-the-art crystal growth facility incorporates two MOCVD reactors, one MBE reactor and a full range of integrated safety equipment. One reactor, purchased from Crystal Specialties Inc., has been specifically assigned to the growth of III-Ns since 1993 and features low pressu re operation, a custom injection manifold to allow flow separation, and a tapered flow channel for high uniformity. The other reactor, purchased from Thomas Swan Ltd., UK, features wafer rotation and is used for the growth of ultra-uniform Ga As, AlGaAs and strained InGaAs structures in support of CHTM research. A commercial, 3 inch Vacuum Generators V80H MBE machine will be used for most of the growth of the AlGaInAs systems to be used in this proposal.

8.2 Characterization Equipments

CHTM has, or has regular access to, a wide range of materials and device characterization equipment that allows us to fully analyze as-grown epitaxial material and optoelectronic or electronic devices. This equipment includes:

For Materials

Transmission Electron Microscopy (resolution 3E);
High Resolution cross-sectional TEM on III-V heterostructures including III-Ns;
Double Crystal X-Ray Rocking Curve Apparatus. (also have access to a single crystal diffractometer;)
Electrochemical C-V profiling of doping concentration;
Photoluminescence (300 K to 4 K) using a range of pulsed and CW laser pump sources, with wavelengths as short as 252 nm;
Hall Mobility Measurements at 600 K to 8 K.

For Devices

Deep Level Transient Spectroscopy (DLTS);
Optical Microscopy, Scanning Electron Microscopy;
Confocal microscopy and confocal photoluminescence with submicron resolution;

Probe station, curve tracer, DC parameter analyzer, and capacitance meter for measurement of I-V and C-V characteristics;
Diode Laser L-I, I-V, and farfield/near-field pattern set-up;
Anritsu Optical Spectrum Analyzer;
HP 50 GHz Network Analyzer and HP 22 GHz Spectrum Analyzer. BER Test Equipment;
CW and pulsed UV lasers for optical pumping including:

1) a quadrupled Nd:YAG laser operating at 266 nm with 10 ns pulses, 10 Hz repetition rate, and 0.25J/pulse peak power;
2) a CW doubled Ar laser operating at 257 nm with peak power of 50 mW;
3) a CW Ar laser operating at 363.8 nm with peak power of 300 mW and
4) an excimer laser capable of 100 ns pulsed operation at 248 nm and 345 nm.
5) femtosecond sources including several Ti:Al2O3 lasers and doubler/tripler wavelength extender

Raman spectroscopy;
Atomic Force Microscopy.

8.3 Semiconductor Processing

CHTM has a fully equipped, 1800 ft2 class-100 clean room for semiconductor materials processing. This clean room is equipped with a JEOL 5800 scanning electron microscope with cathodluminescence and x-ray analysis, a wet chemical etching aisle, a solvent cleaning aisle, a photolithography bay, and features a Plasma Quest electron cyclotron resonance (ECR) reactive ion etcher, four e-beam evaporation systems for metallization and optical coatings, PECVD and LPCVD for dielectric deposition, a barrel asher, two rapid thermal annealers , an ellipsometer, and a surface profilometer. Device processing is based on g-line contact photolithography with either positive or negative photo-resist technology.

8.4 Equipment to be purchased

We plan to purchase a dedicated monchromator and photon counting system so as to aleviate overcrowding on the current system. In addition, because of the growth intensive nature of this program, spare MBE parts are budgeted for in terms of a replacment Knudsen cell.